Eur Biophys J (2006) 35:611–620
DOI 10.1007/s00249-006-0074-6

ARTICLE

Neutron Laue macromolecular crystallography

Flora Meilleur · Dean A. A. Myles · Matthew P. Blakeley

Received: 27 February 2006 / Revised: 27 April 2006 / Accepted: 4 May 2006 / Published online: 3 August 2006

Abstract Recent progress in neutron protein crystallography such as the use of the Laue technique and improved neutron optics and detector technologies have dramatically improved the speed and precision with which neutron protein structures can now be determined. These studies are providing unique and complementary insights on hydrogen and hydration in protein crystal structures that are not available from X-ray structures alone. Parallel improvements in modern molecular biology now allow fully (per)deuterated protein samples to be produced for neutron scattering that essentially eradicate the large—and ultimately limiting—hydrogen incoherent scattering background that has hampered such studies in the past. High quality neutron data can now be collected to near atomic resolution (~2.0 Å) for proteins of up to ~50 kDa molecular weight using crystals of volume ~0.1 mm^3 on the Laue diffractometer at ILL. The ability to flash-cool and collect high resolution neutron data from protein crystals at cryogenic temperature (15 K) has opened the way for kinetic crystallography on freeze trapped systems. Current instrument developments now promise to reduce crystal volume requirements by a further order of magnitude, making neutron protein crystallography a more accessible and routine technique.

F. Meilleur (✉)
Institut Laue Langevin, BP 156,
38042 Grenoble Cedex 9, France
e-mail: meilleur@ill.fr

D. A. A. Myles
Oak Ridge National Laboratory, P.O. Box 2008,
Oak Ridge, TN 37831, USA

M. P. Blakeley
European Molecular Biology Laboratory,
BP 181, 38042 Grenoble, France

Introduction

Hydrogen can be visualized in electron density maps calculated from X-ray crystallographic analyses if ultra-high resolution (<1.0 Å) data are available (Dauter et al. 1997; Longhi et al. 1998; Schmidt et al. 2002; Schmidt et al. 2003; Podjarny et al. 2004). There are currently ~30,000 X-ray protein structures deposited to the Protein Data Bank (http://www.rcsb.org) of which ultra-high resolution structures represent less than 1%. Such resolutions are generally reached for modest size macromolecules (75% are less than 200 residues) and/or small unit cell parameter crystals (85% have at least one unit cell parameter smaller than 90 Å). Moreover, even when such data can be collected, the visibility of individual hydrogen atoms can be hampered by the degree of thermal motion (B-factors>10 $Å^2$) (Howard et al. 2004). Water hydrogen atoms or hydrogen at the active site of an enzyme therefore can be difficult to visualize.

In contrast, neutron crystallography is able to localize hydrogen positions in protein structures at 1.5–2.0 Å resolutions. This is because neutrons are scattered by the nuclei of the atoms in the crystal lattice, whereas X-rays are scattered by the electron clouds. As a consequence, X-ray scattering amplitudes are proportional to the number of electrons of the atoms,

Table 1 Neutron coherent scattering lengths and incoherent cross-section and X-ray scattering factors in biological materials

Isotope	Abundance (%)	Atomic Number	Neutron incoherent cross section (Barns)	Neutron coherent scattering length (10^{-12} cm)	X-ray scattering factors (10^{-12} cm)	
					$\sin\theta = 0$	$(\sin\theta)/\lambda = 0.5$ Å^{-1}
^{1}H	99.985	1	80.27	–0.374	0.28	0.02
^{2}H (D)	0.015		2.05	0.667	0.28	0.02
^{12}C	98.9	6	0.00	0.665	1.69	0.48
^{14}N	99.63	7	0.49	0.937	1.97	0.53
^{16}O	99.762	8	0.00	0.580	2.25	0.62
^{24}Mg	78.99	12	0.00	0.549	3.38	1.35
^{32}S	95.02	16	0.00	0.280	4.50	1.90
^{39}K	93.258	19	0.25	0.379	5.30	2.20
^{55}Mn	100	25	0.40	–0.375	7.00	3.10
^{56}Fe	91.7	26	0.00	1.012	7.30	3.30

while the neutron scattering amplitudes (neutron scattering length, b) depends on the nuclear forces, which vary between elements and even between isotopes of the same element. Another important aspect of neutron scattering is that the total scattering by a nucleus is the sum of two terms, namely the coherent and the incoherent scattering. It is the coherent scattering that gives rise to interference, hence to Bragg peaks, while the incoherent scattering, which is isotropically distributed, is the major source of background in neutron crystallography experiments. The extent of incoherent scattering is determined by the spin state of the target nuclei. The neutron coherent scattering lengths and X-ray scattering factors for some elements found in biological macromolecules are presented in Table 1. Positive values of neutron scattering length b reflect a 180° change in phase between the incident and the scattered neutron waves. Negative values of b are associated with a resonance level that produces an extra 180° phase shift (Korszun 1997). The neutron scattering length b is essentially constant as a function of $(\sin\theta)/\lambda$ because the dimensions of an atomic nucleus are significantly smaller than the wavelength of the neutrons used in diffraction experiments, while X-ray scattering factors drop rapidly as $(\sin\theta)/\lambda$ increases (Fig. 1).

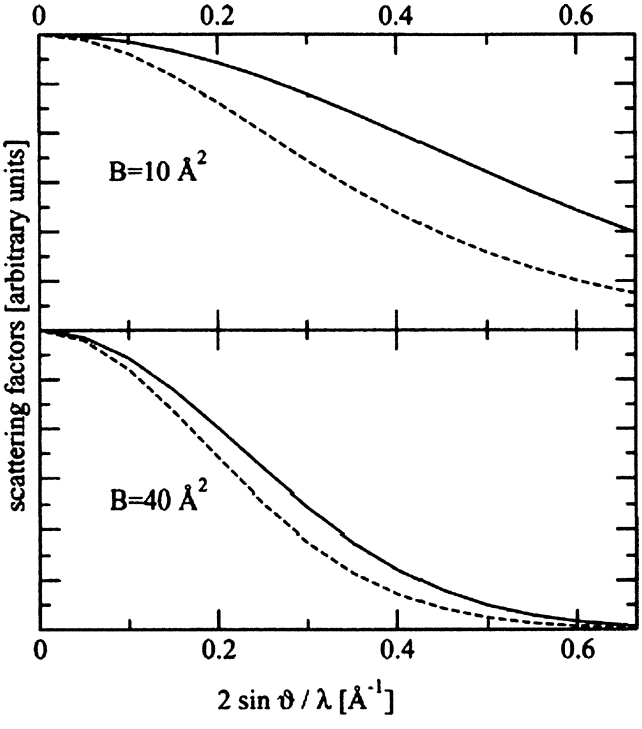

Fig. 1 Comparison of the X-ray atomic scattering factors (*dashed line*) and neutron scattering lengths (*straight line*) as a function of scattering angle with the influence of thermal motion (from Ostermann et al. 2002)

There is considerably less variation across the periodic table in the case of neutron scattering lengths than for X-ray scattering factors. The most striking illustration of this is that hydrogen and its isotope deuterium have similar scattering lengths to the other ''heavy'' atoms found in a protein, namely carbon, oxygen and nitrogen (Table 1). Therefore the position of hydrogen atoms can be assigned as readily as the position of the other atoms using neutron crystallography even at the 1.5–2.0 Å resolution limits typical of most protein structures.

Neutron macromolecule crystallography

The high visibility of H/D atoms and of water (D_2O) in neutron protein structures makes neutron crystallography highly complementary to X-ray crystallography in cases where specific biological questions such as understanding catalytic mechanisms require knowledge of the exact location of hydrogen atoms in enzyme structures or to better describe the solvent structure in and surrounding proteins.

Despite its obvious potential, the use of neutron crystallography has previously been limited by the inherent low fluxes of even the most powerful neutron sources. As a result, only a handful of neutron protein structures have thus far been determined. Table 2 lists the ensemble of macromolecules for which a neutron structure has been deposited in the Protein Data Bank or those currently being refined.

A common requirement—and limitation—of neutron protein crystallography is the need for unusually large crystal volumes required (Table 2). This is primarily due to the weak flux of available neutron beams. The diffracted intensity in Bragg

Table 2 Protein crystals for which neutron data have been collected, sorted by ascending $V/(v_0)^2$ ratio, where V is the volume of the crystal measured and v_0 the volume of the primitive crystallographic unit cell (cf. Eq. 1). *LADI* Laue Diffractometer. *PCS* Protein crystallography station. *BIX* Neutron diffractometer for biology. *CD* Conventional diffractometer

Protein	Instrument	Unit cell volume v_0 (Å^3)	Crystal size V (mm^3)	$V/(v_0)^2$ (10^9 Å^{-3})	Resolution (Å)	Reference
Dihydrofolate reductase	LADI	518136	0.3	1.1	2.2	Bennett et al. (2005)
Perdeuterated Aldose reductase	LADI	161535	0.15	5.7	2.2	Hazemann et al. (2005)
Urate oxidase	LADI	407036	1.8	10.1	2.1	Budayova-Spano et al. (2006)
15K Concanavalin A	LADI	472971	1.6/5.6	7/25	2.5	Blakeley et al. (2004)
D-xylose isomerase	PCS	480230	5	21.6	2.0	Hanson et al. (2004)
D-xylose isomerase	LADI	463424	8	37	2.2	Meilleur et al. (2006)
Dissimilatory sulfite reductase D	BIX	183142	1.7	51	2.4	Chatake et al. (2004)
Concanavalin A	LADI	479534	15	65	2.4	Habash et al. (2000)
Insulin	CD	200409	3.4	84	2.2	Wlodawer et al. (1989)
Lysozyme	LADI	228999	6	114	2.0	Niimura et al. (1997a, b)
Trp repressor	LADI	93420	1.12	130	2.1	Daniels et al. (2003)
Endothiapepsin	LADI	158139	3.5	140	2.0	Cooper et al. (2000)
B-DNA decamer	BIX	104020	2.8/1.6	259/148	3.0	Arai et al. (2005)
Insulin	BIX	245771	20.8	344	1.6	Maeda et al. (2004)
15 K Rubredoxin	LADI	53500	1.4	489	1.7	Blakeley et al. unpublished
Perdeuterated Myoglobin	CD	64216	2.5	606	2.0	Shu et al. (2000)
Trypsin	CD	50111	1.6	637	2.2	Kossiakoff et al. (1981)
Z-DNA	PCS	25172	0.7	1105	1.6	Langan et al. (2006)
Rubredoxin	PCS	53600	4	1390	2.1	Li et al. (2004)
Amicyanin	PCS	43127	2.6	1400	1.9	Sukumar et al. (2005)
Myoglobin	BIX	64464	6.25	1500	1.5	Engler et al. (2003)
Rubredoxin	BIX	53516	5	1750	1.5	Bau (2004)
Rubredoxin	BIX	53207	5	1760	1.6	Chatake et al. (2003)
Oxymyoglobin	CD	64500	8	1920	2.0	Phillips et al. (1981)
Z-DNA hexameric duplex	BIX	24519	1.6	2660	1.6	Chatake et al. (2005)
Lysozyme	LADI	22771	2	3860	1.7	Bon et al. (1999)
Crambin	CD	17155	1.4	4760	1.5	Teeter et al. (1984)
Metmyoblobin	CD	64500	24	5760	2.0	Raghavan et al. (1984)
Carbon-momoxymyoglobin	CD	64501	24	5770	1.8	Cheng et al. (1991)
15 K Lysozyme	LADI	22771	4	7710	1.6	Meilleur et al. (2005)
Ribonuclease A	CD	57228	30	9160	2.0	Wlodawer et al. (1984)
Lysozyme	CD	22771	20	38570	1.4	Mason et al. (1984)

reflections in a single crystal experiment can be written as:

$$I = I_0 \cdot F^2 \cdot V \cdot A/(v_0)^2 \quad (1)$$

where I, I_0, F, V, A, and v_0 are the diffracted intensity, incident neutron intensity, structure factor, volume of the crystal, detector area subtended by the sample and volume of the unit cell, respectively (Niimura 1999). While ~10^{10} photons $cm^{-2}s^{-1}$ are available from rotating anodes or ~10^{16} photons $cm^{-2}s^{-1}$ from synchrotrons, the neutron flux I_0 at the sample position ranges from 10^6 to 10^9 neutrons $cm^{-2}s^{-1}$ (~3×10^7 on the LAue DIffractomer LADI) even at the most intense neutron sources.

Historically, this resulted in very long data collection times and time scales for data collection were often prohibitive. This also was due in part to the lack of dedicated, optimized instrumentation for macromolecular crystallography. In conventional instruments, the incident neutron beam was monochromatized, and the data measured on four-circle diffractometers or flat-cone diffractometers (Wlodawer et al. 1989) composed of a moveable detector that is sequentially positioned to record each Bragg reflection individually. As a consequence, neutron macromolecule crystallographic studies were limited to crystals of generally low molecular weight proteins (<20 kDa), with small unit cell parameters (<50 Å) (Table 2) and for which crystals of unusually large volume could be grown [i.e., cases for which $V/(v_0)^2$ is favorable (Eq. 1)]. More recent advances in both instrumentation and sample preparation have lowered both data collection times and the crystal volume requirements, greatly extending the range of problems that are accessible to the technique. Instruments at reactor (Kurihara et al. 2004; Myles et al. 1998) and spallation (Schoenborn and Langan 2004) sources have been optimized in order to maximize the flux of neutrons at the sample and have improved detector efficiencies and larger angular coverage. One measure of the advances provided by this current suite of instruments is in the dramatic reduction of the ratio of $V/(v_0)^2$ (Eq.1) required for successful neutron analysis of larger unit cell systems (Fig. 2).

The LAue DIffractometer (LADI) at the Institut Laue Langevin

At the Institut Laue Langevin, the neutron Laue diffractometer LADI was developed in order to speed up

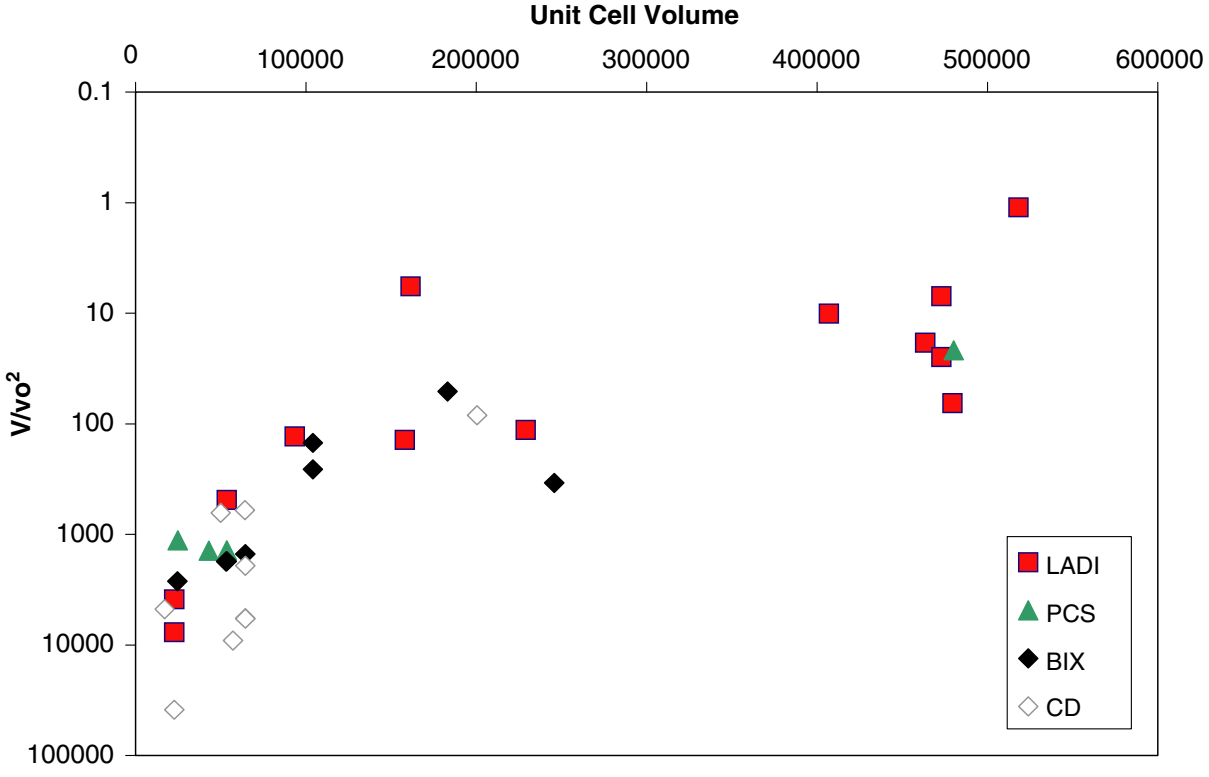

Fig. 2 Plot showing the ratio of $V/(v_0)^2$ (10^9 $Å^{-3}$) as a function of the primitive unit cell volume, v_0, where V ($Å^3$) is the volume of the crystal from which neutron data have been measured (cf. Eq. 1), *LADI* laue diffractometer. *PCS* Protein crystallography station. *BIX* neutron diffractometer for biology. *CD* conventional diffractometer

data collection and allow smaller crystals to be measured (Cipriani et al. 1994, 1996; Myles et al. 1998). The LADI instrument (Fig. 3) is dedicated to protein crystallography. Two key changes were made in the experimental design compared to diffractometers previously used: (1) a large cylindrical area detector made of neutron-sensitive image plates was designed, surrounds the sample and allows many stimulated Bragg reflections to be recorded simultaneously; (2) the Laue (white beam) method is used to provide a more rapid and efficient survey of reciprocal space, maximizing the flux on the sample by using all available neutrons within a broad spectral range and stimulating very large numbers of reflections at all possible wavelengths over many different angles (Myles 2003). For crystal with unit cell parameter greater than 50 Å—typical of most biological crystals, where use of the full white beam can cause many of the stimulated reflections to be overlapped at the detector, a more limited wavelength bandpass (quasi-Laue) is preferred. In such cases, a Ni/Ti multilayer filter is used to select the wavelength range ($\Delta\lambda/\lambda$) and wavelength (λ) that is best suited to the sample (Høghøj et al. 1996). A λ = 3.5 Å, $\Delta\lambda/\lambda$ ~25%, is used for most applications. The resolution then at the edge of the detector is ~1.5 Å, sufficient to localize hydrogen/deuterium atoms. Further advantages of using a restricted wavelength bandpass are that the background on the detector is reduced proportionally compared to the Laue technique, the number of energy overlapped harmonic reflections is significantly reduced and that almost all reflections (>99%) recorded are single. These combined improvements have greatly accelerated data collection rates (Helliwell 1997; Myles et al. 1998) thus making smaller crystals and larger systems accessible to neutron crystallography (Table 2). For example, data collection on LADI for standard systems such as lysozyme (Niimura et al. 1997a, b; Bon et al. 1999) has been performed with an order of magnitude acceleration in the data collection rate over conventional diffractometers. Data have also been collected in 2–3 weeks for larger systems such as concanavalin A (Habash et al. 2000; Blakeley et al. 2004), Trp repressor (Daniels et al. 2003), endothiapepsin (Cooper and Myles 2000; Coates et al. 2001), aldose reductase (Hazemann et al. 2005), dihydrofolate reductase (Bennett et al. 2005), xylose isomerase (Meilleur et al. 2006) and urate oxidase (Budayova-Spano et al. 2006). Some details of the neutron structures refined against LADI data are shown on Fig. 4.

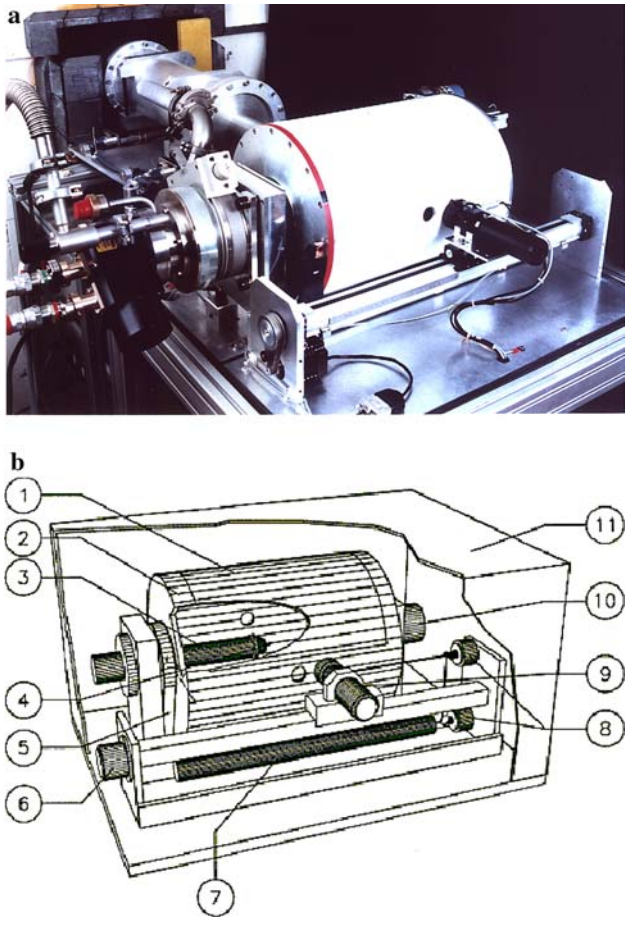

Fig. 3 **a** The Laue DIffractometer at ILL (cover removed) **b** (from Cipriani et al. 1996). *1* Neutron-sensitive image plate on drum. *2* Drum. *3* Sample holder. *4* Crystal. *5* Transmission belt to drive drum. Motor is under table. *6* Carrier for reading head with photomultiplier. *7* He–Ne laser. *8* Mirrors for bringing the laser light to the reader head. *9* Reader head with photomultiplier. *10* Encoder for drum rotation. *11* Cover

Perdeuteration

Hydrogen has a large incoherent cross section (Table 1). Whilst this incoherent signal can be exploited to provide dynamic information in inelastic neutron scattering experiments, in diffraction experiments the large hydrogen incoherent scattering gives rise to a large and significant background. As hydrogen atoms account for about 50% of the atoms in a protein and are also present in the surrounding H_2O solvent molecules, the signal to noise ratio of neutron diffraction data from fully hydrogenated systems is dominated by the large incoherent background. Moreover, due to their negative scattering length, hydrogen atoms appear as negative density in neutron Fourier maps, in contrast to the other elements, including deuterium, which appear as positive density peaks. Whilst this difference in sign between hydrogen and deuterium

neutron density can be exploited to give information on solvent accessibility of the target groups in a protein (H/D exchange), it may also unfortunately lead to neutron density cancellation around neighboring atoms (at the ~2.0 Å resolutions typical of these experiments) hampering accurate interpretation of the resulting neutron maps (Shu et al. 2000). In contrast, the incoherent scattering arising from deuterium is 40 times lower, whilst the neutron scattering length is positive and twice that of hydrogen (Table 1). Therefore

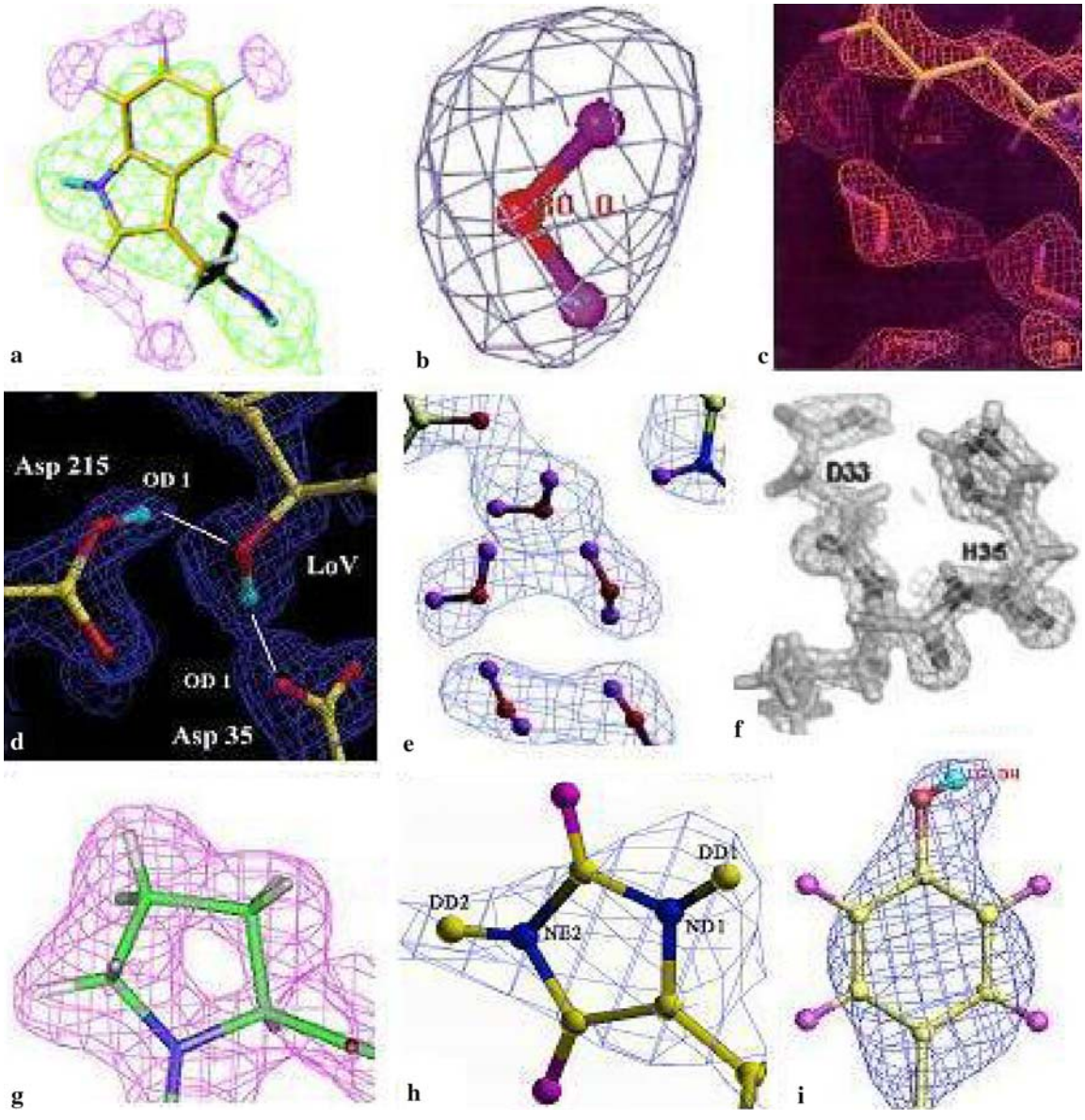

Fig. 4 Details from neutron structures refined against LADI data. **a** Visualization of hydrogen and deuterium atom in lysozyme at 2.0 Å resolution. Green $2F_o–F_c$ positive neutron density map; pink $2F_o–F_c$ negative neutron density map (from Niimura et al. 1997a, b). **b** Orientation of a water molecule in concanavalin A with room temperature LADI data at 2.4 Å. $2F_o–F_c$ neutron density map contoured at 1.5σ (from Habash et al. 2000). **c** Hydration shells around lysozyme at room temperature using 1.7 Å resolution data. $2F_o–F_c$ neutron density map, omitting the water molecule and contoured at the 1σ (from Bon et al. 1999). **d** Location of hydrogen/deuterium atom at the active site of endothiapepsin in a 2.1 Å resolution LADI structure (from Coates et al. 2001). **e** Increased visibility of water molecules in concanavalin A using cryogenic data at 2.5 Å resolution. $2F_o–F_c$ neutron map contoured at 1.5σ (from Blakeley et al. 2004). **f** Hydrogen deuterium exchange in Trp repressor (from Lawson and Chin 2003). **g** Enhanced visibility of hydrogen atoms in fully deuterated human aldose reductase at 2.2 Å resolution. $2F_o–F_c$ neutron density map contoured at 1.5σ (from Hazemann et al. 2005). **h** Histidine protonation state at the active site of D-xylose isomerase in a 2.2 Å neutron structure. $2F_o–F_c$ neutron map contoured at 1.5σ (from Meilleur et al. 2006). **i** Orientation of hydroxyl group in the 2.1 Å resolution neutron structure of urate oxidase in complex with 8-azaxanthin. $2F_o–F_c$ neutron density map contoured at 1.5σ (from Budayova-Spano et al. 2006)

replacing hydrogen by deuterium in protein crystals increases the coherent scattering signal and decreases the incoherent background, typically providing a near order of magnitude improvement of the signal to noise ratio of the data. Deuterium labeling can be achieved either partially, by soaking crystals in deuterated mother liquor, or more fully, by preparing completely (per)deuterated protein samples. In addition to the replacement of the bulk solvent and of hydration waters, exchange with deuterated solvent results in about 15 to 20% of the solvent accessible hydrogen content of the protein being exchanged for deuterium, i.e., hydrogen atoms that are bound to nitrogen or oxygen (amino and hydroxyl groups). This approach has been used successfully in a number of LADI experiments (Bon et al. 1999; Cooper et al. 1999; Habash et al. 2000; Blakeley et al. 2004; Bennett et al. 2005; Budayova-Spano et al. 2006; Snell et al. 2006) (Table 2). In order to replace the remaining hydrogen atoms which are bound to carbon, it is necessary to express the protein under deuterated conditions in vivo. Fully deuterated systems offer as much as a 40-fold reduction in the background (Gamble et al. 1994) and thus enables radically smaller crystals to be used for neutron data collection. This has been recently demonstrated in the case of aldose reductase, for which neutron data to 2.2 Å resolution were collected from a 0.15 mm^3 (Table 2) perdeuterated aldose reductase crystal (Hazemann et al. 2005; Blakeley et al. 2006). Since the growth of very large single crystals has been a major hurdle in neutron protein crystallography, this result demonstrates the critical advance offered by perdeuteration. Moreover, studies have shown that the structural features of fully deuterated proteins are not significantly altered at the resolution of the analyses (Gamble et al. 1994; Cooper et al. 1998; Tuominen et al. 2004; Meilleur et al. 2005; Artero et al. 2006; Budayova-Spano et al. 2006), validating the use of perdeuterated protein in neutron protein crystallography. Facilities dedicated to the production of deuterated macromolecules are now available at the Institut Laue Langevin and European Molecular Biology Laboratory in Grenoble, and at Los Alamos (PCS) and Oak Ridge (CSMB) national laboratories.

Cryo-neutron crystallography

Neutrons do not cause any observable radiation damage in protein crystals and thus most experiments are performed at room temperature. However, cryo-cooling protein crystals in X-ray crystallography has been shown (in some cases) to provide improvements in data quality by reducing B-factors, and also opens up possibilities for freeze trapping studies of enzymatic reaction intermediates. This is challenging for large protein crystals since the solvent must be rapidly (flash)-cooled to a vitreous glass in order to avoid ice formation that disrupts the crystal lattice. Protocols for cryo neutron crystallography have been developed to cool and maintain large protein crystals (1–5 mm^3) at cryogenic temperatures (< 15 K) and have provided neutron diffraction data to high-resolution (~1.5–2.5 Å). Data have been collected for lysozyme (Myles et al. 2003; Meilleur et al. 2005), concanavalin A (Blakeley et al. 2004) and rubredoxin (M.P. Blakeley et al. in preparation). In each case, crystals were mounted in fiber loops, passed rapidly through glycerol cryo-protectant solutions, and then flash-cooled by plunging directly into liquid N_2 (77 K). The crystals were then transferred under liquid N_2 and mounted and cooled to 15 K on the cold head of a displex cryostat custom built for LADI. These results open up new experimental capabilities that will allow analysis of structure (and transitions) as a function of temperature and the ability to use freeze trapping to 'quench' kinetic processes and capture reaction intermediaries, allowing new scientific questions to be addressed.

Conclusion and perspectives

Recent progress in neutron protein crystallography such as the use of the Laue technique and improved neutron optics and detector technologies have dramatically improved the speed and precision with which neutron protein structures can now be determined. These studies are providing unique and complementary insights on hydrogen and hydration in protein crystal structures that are not available from X-ray structures alone. Parallel improvements in modern molecular biology now allow fully (per)deuterated protein samples to be produced for neutron scattering that essentially eradicate the large—and ultimately limiting—hydrogen incoherent scattering background that has hampered such studies in the past. High quality neutron data can now be collected to near atomic resolution (~2.0 Å) for proteins of up to ~50 kDa molecular weight using crystals of volume ~0.1 mm^3 on the Laue diffractometer at ILL. The ability to flash-cool and collect high resolution neutron data from protein crystals at cryogenic temperature (15 K) now opens the way for kinetic crystallography on freeze trapped systems.

However, neutron protein crystallography still remains a demanding and intensity limited technique. Experiments still fall just at the edge of feasibility, frustrated by the size of the available crystals. A further order of magnitude gain in capability would be decisive in extending the range, scale and complexity of problems that are accessible to neutron analysis. This is being addressed at new neutron sources and facilities worldwide. At ILL, the LADI instrument has been redesigned and a new instrument is under construction. Measurements suggest that transferring the image plates and readout system to the inside of the drum will provide a threefold gain in neutron detection efficiency (Myles et al. 2000; Wilkinson et al. unpublished work). In addition, the dimensions of the drum have been increased to 400 mm in diameter and 450 mm in length (current LADI is 320 mm in diameter and 400 mm in length), which will help resolve spatially overlapped Bragg reflections and reduce the isotropic background scatter per pixel at the detector. The upgraded diffractometer will come on line in 2006 and combined with its re-location on a new high intensity neutron guide, should provide a further order of magnitude improvement in performance.

The development of time-of-flight protein diffractometers at the new intense spallation neutron source (SNS) in the USA and at a similar facility in Japan offer the promise of yet further 10–50-fold gains in performance. The major advantage of these instruments is that whilst a very broad (Laue) band-pass is used, the pulsed time structure and energy resolution of the incident neutron beam reduces the number of both harmonic and spatially overlapped reflections and improves the signal-to-noise ratio of the data (Schultz et al. 2005). Such gains in performance can be expected to significantly extend the size and complexity of systems that can be studied by neutron crystallography.

Acknowledgments DAAM acknowledges support in part under DOE contract No. DE-AC05-00OR22725 with Oak Ridge National Laboratory, managed and operated by UT-Batelle, LLC.

References

Arai S, Chatake T, Ohhara T, Kurihara K, Tanaka I, Suzuki N, Fujimoto Z, Mizuno H, Niimura N (2005) Complicated water orientations in the minor groove of the B-DNA decamer d(CCATTAATGG)2 observed by neutron diffraction measurements. Nucleic Acids Res 33(9):3017–3024

Artero JB, Hartlein M, McSweeney S, Timmins P (2006) A comparison of refined X-ray structures of hydrogenated and perdeuterated rat gammaE-crystallin in H2O and D2O. Acta Crystallogr D Biol Crystallogr 61(Pt 11):1541–1549

Bau R (2004) Neutron diffraction studies on rubredoxin from Pyrococcus furiosus. J Synchrotron Radiat 11(Pt 1):76–79

Bennett BC, Myles DA, Howell EE, Dealwis CG (2005) Preliminary neutron diffraction studies of Escherichia coli dihydrofolate reductase bound to the anticancer drug methotrexate. Acta Crystallogr D Biol Crystallogr 61(Pt 5):574–579

Blakeley MP, Mitschler A, Hazemann I, Meilleur F, Myles DA, Podjarny A (2006) Comparison of hydrogen determination with X-ray and neutron crystallography in a human aldose reductase-inhibitor complex. Eur Biophys J(this issue)

Blakeley MP, Kalb AJ, Helliwell JR, Myles DA (2004) The 15-K neutron structure of saccharide-free concanavalin A. Proc Natl Acad Sci USA 101(47):16405–16410

Bon C, Lehmann MS, Wilkinson C (1999) Quasi-Laue neutron-diffraction study of the water arrangement in crystals of triclinic hen egg-white lysozyme. Acta Crystallogr D Biol Crystallogr 55(Pt 5):978–987

Budayova-Spano M, Bonneté F, Ferté N, El Hajji M, Meilleur F, Blakeley MP, Castro B (2006) Acta Crystallogr F Biol Crystallogr 62:306–309

Budayova-Spano M, Fisher SZ, Dauvergne MT, Agbandje-McKenna M, Silverman DN, Myles DA, McKenna R (2006) Production and X-ray crystallographic analysis of fully deuterated human carbonic anhydrase II. Acta Crystallograph Sect F Struct Biol Crystallogr 62(Pt 1):6–9

Chatake T, Tanaka I, Umino H, Arai S, Niimura N (2005) The hydration structure of a Z-DNA hexameric duplex determined by a neutron diffraction technique. Acta Crystallogr D Biol Crystallogr 61(Pt 8):1088–1098

Chatake T, Ostermann A, Kurihara K, Parak FG, Mizuno N, Voordouw G, Higuchi Y, Tanaka I, Niimura N (2004) Hydration structures in proteins and neutron diffraction experiment on dissimilatory sulfite reductase D (DsrD). J Synchrotron Radiat 11(Pt 1):72–75

Chatake T, Ostermann A, Kurihara K, Parak FG, Niimura N (2003) Hydration in proteins observed by high-resolution neutron crystallography. Proteins 50(3):516–523

Cheng XD, Schoenborn BP (1991) Neutron diffraction study of carbonmonoxymyoglobin. J Mol Biol 220(2):381–399

Cipriani F, Dauvergne F, Gabriel A, Wilkinson C, Lehmann MS (1994) Image plate detectors for macromolecular neutron diffractometry. Biophys Chem 53:5–13

Cipriani F, Castagna JC, Wilkinson C, Lehmann MS, Buldt G (1996) A neutron image plate quasi-Laue diffractometer for protein crystallography. Basic Life Sci 64:423–431

Coates L, Erskine PT, Wood SP, Myles DA, Cooper JB (2001) A neutron Laue diffraction study of endothiapepsin: implications for the aspartic proteinase mechanism. Biochemistry 40(44):13149–13157

Cooper JB, Myles DA (2000) A preliminary neutron Laue diffraction study of the aspartic proteinase endothiapepsin. Acta Crystallogr D Biol Crystallogr 56(Pt 2):246–248

Daniels BV, Myles DA, Forsyth VT, Lawson CL (2003) Crystals of Trp repressor suitable for high-resolution neutron Laue diffraction studies. Acta Crystallogr D Biol Crystallogr 59(Pt 1):136–138

Dauter Z, Lamzin VS, Wilson KS (1997) The benefits of atomic resolution. Curr Opin Struct Biol 7(5):681–688

Engler N, Ostermann A, Niimura N, Parak FG (2003) Hydrogen atoms in proteins: positions and dynamics. Proc Natl Acad Sci USA 100(18):10243–10248

Habash J, Raftery J, Nuttall R, Price HJ, Wilkinson C, Kalb AJ, Helliwell JR (2000) Direct determination of the positions of the deuterium atoms of the bound water in-concanavalin A

by neutron Laue crystallography. Acta Crystallogr D Biol Crystallogr 56 (Pt 5):541–50

Hanson BL, Langan P, Katz AK, Li X, Harp JM, Glusker JP, Schoenborn BP, Bunick GJ (2004) A preliminary time-of-flight neutron diffraction study of Streptomyces rubiginosus D-xylose isomerase. Acta Crystallogr D Biol Crystallogr 60(Pt 2):241–249

Hazemann I, Dauvergne MT, Blakeley MP, Meilleur F, Haertlein M, Van Dorsselaer A, Mitschler A, Myles DA, Podjarny A (2005) High-resolution neutron protein crystallography with radically small crystal volumes: application of perdeuteration to human aldose reductase. Acta Crystallogr D Biol Crystallogr 61(Pt 10):1413–1417

Helliwell JR (1997) Neutron Laue diffraction does it faster. Nat Struct Biol 4(11):874–876

Høghøj P, Anderson IS, Ebisawa T, Takeda T (1996) Fabrication and performance of a large wavelength band multilayer monochromator. J Phys Soc Jpn 65:296–298

Howard EI, Sanishvili R, Cachau RE, Mitschler A, Chevrier B, Barth P, Lamour V, Van Zandt M, Sibley E, Bon C, Moras D, Schneider TR, Joachimiak A, Podjarny A (2004) Ultrahigh resolution drug design I: details of interactions in human aldose reductase-inhibitor complex at 0.66 A. Proteins 55(4):792–804

Korszun ZR (1997) Neutron macromolecular crystallography. Methods Enzymol 276: 219–232

Kossiakoff AA, Spencer SA (1981) Direct determination of the protonation states of aspartic acid-102 and histidine-57 in the tetrahedral intermediate of the serine proteases: neutron structure of trypsin. Biochemistry 20(22):6462–6474

Kurihara K, Tanaka I, Niimura N, Refai Muslih M, Ostermann A (2004) A new neutron single-crystal diffractometer dedicated for biological macromolecules (BIX-4). J Synchrotron Radiat 11:68–71

Langan P, Li X, Hanson BL, Coates L, Mustyakimov M (2006) Synthesis, capillary crystallization and preliminary joint X-ray and neutron crystallographic study of Z-DNA without polyamine at low pH. Acta Crystallogr F Biol Crystallogr 62

Lawson CL, Chin AS (2003) Analysis of neutron Laue diffraction from deuterium-exchanged Trp-repressor. Transactions ACA 38

Longhi S, Czjzek M, Cambillau C (1998) Messages from ultrahigh resolution crystal structures. Curr Opin Struct Biol 8(6):730–737

Li X, Langan P, Bau R, Tsyba I, Jenney FE Jr, Adams MW, Schoenborn BP (2004) W3Y single mutant of rubredoxin from Pyrococcus furiosus: a preliminary time-of-flight neutron study. Acta Crystallogr D Biol Crystallogr 60(Pt 1): 200–202

Maeda M, Chatake T, Tanaka I, Ostermann A, Niimura N (2004) Crystallization of a large single crystal of cubic insulin for neutron protein crystallography. J Synchrotron Radiat 11(Pt 1):41–44

Mason SA, Bentley GA, McIntyre GJ (1984) Deuterium exchange in lysozyme at 1.4-A resolution. Basic Life Sci 27:323–234

Meilleur F, Snell EH, van der Woerd MJ, Judge RA, Myles DA (2006) A quasi-Laue neutron crystallographic study of D-xylose isomerase. Eur Biophys J (this issue)

Meilleur F, Blakeley MP, Myles DA (2005) Neutron Laue analysis of hydrogen and hydration in protein structure. In: Niimura N., Mizuno H., Helliwell J.R., Westhof E, (Eds) Hydrogen and hydration sensitive structural biology. pp 75–85

Meilleur F, Dauvergne MT, Schlichting I, Myles DA (2005) Production and X-ray crystallographic analysis of fully deuterated cytochrome P450cam. Acta Crystallogr D Biol Crystallogr 61(Pt5):539–544

Myles DA, Bon C, Langan P, Cipriani F, Castagna JC, Lehmann MS, Wilkinson C (1998) Neutron Laue diffraction in macromolecular crystallography. Physica B 241–243:1122–1130

Myles DA, Timmins PA, Wilkinson C (2000) ILL Millenium Programme, Document ILL01CA01T, pages 42–45

Myles DA (2003) Recent trends and advances in neutron macromolecular crystallography. Transactions ACA 38

Niimura N, Minezaki Y, Nonaka T, Castagna JC, Cipriani F, Hoghoj P, Lehmann MS, Wilkinson C (1997a) Neutron Laue diffractometry with an imaging plate provides an effective data collection regime for neutron protein crystallography. Nat Struct Biol 4(11):909–914

Niimura N (1999) Neutrons expand the field of structural biology. Curr Opin Struct Biol 9(5):602–608

Niimura N, Minezaki Y, Nonaka T, Castagna JC, Cipriani F, Hoghoj P, Lehmann MS, Wilkinson C (1997b) Neutron Laue diffractometry with an imaging plate provides an effective data collection regime for neutron protein crystallography. Nat Struct Biol 4(11):909–914

Ostermann A, Tanaka I, Engler N, Niimura N, Parak FG (2002) Hydrogen and deuterium in myoglobin as seen by a neutron structure determination at 1.5 Å resolution. Biophys Chem 95(3):183–193

Phillips SE, Schoenborn BP (1981) Neutron diffraction reveals oxygen-histidine hydrogen bond in oxymyoglobin. Nature 292(5818):81–82

Podjarny A, Cachau RE, Schneider T, Van Zandt M, Joachimiak A (2004) Subatomic and atomic crystallographic studies of aldose reductase: implications for inhibitor binding. Cell Mol Life Sci 61(7–8):763–773

Raghavan NV, Schoenborn BP (1984) The structure of bound water and refinement of acid metmyoglobin. Basic Life Sci 27:247–259

Schmidt A, Lamzin VS (2002) Veni, vidi, vici - atomic resolution unravelling the mysteries of protein function. Curr Opin Struct Biol 12(6):698–703

Schmidt A, Jelsch C, Ostergaard P, Rypniewski W, Lamzin VS (2003) Trypsin revisited: crystallography AT (SUB) atomic resolution and quantum chemistry revealing details of catalysis. J Biol Chem 278(44):43357–43362

Schoenborn BP, Langan P (2004) Protein crystallography with spallation neutrons. J Synchrotron Radiat 11:80–82

Schultz AJ, Thiyagarajan P, Hodges JP, Rehm C, Myles DA, Langan P, Mesecar AD (2005) Design of the next generation neutron macromolecular diffractometer (MaNDi) at the Spallation Neutron Source. J Appl Cryst 38:964–974

Shu F, Ramakrishnan V, Schoenborn BP (2000) Enhanced visibility of hydrogen atoms by neutron crystallography on fully deuterated myoglobin. Proc Natl Acad Sci USA 97(8):3872–3877

Snell EH, van der Woerd MJ, Damon M, Judge RA, Myles DA, Meilleur F (2006) Optimizing crystal volume for neutron diffraction: Xylose Isomerase. Eur Biophys J, this issue

Sukumar N, Langan P, Mathews FS, Jones LH, Thiyagarajan P, Schoenborn BP, Davidson VL (2005) A preliminary time-of-flight neutron diffraction study on amicyanin from Paracoccus denitrificans. Acta Crystallogr D Biol Crystallogr 61(Pt 5):640–642

Teeter MM, Kossiakoff AA (1984) The neutron structure of the hydrophobic plant protein crambin. In: Schoenborn B (ed) Neutrons in Biology. Plenum Press, New York, pp 335–348

Tuominen VU, Myles DA, Dauvergne MT, Lahti R, Heikinheimo P, Goldman A (2004) Production and preliminary

analysis of perdeuterated yeast inorganic pyrophosphatase crystals suitable for neutron diffraction. Acta Crystallogr D Biol Crystallogr 60(Pt 3):606–609

Wlodawer A, Savage H, Dodson G (1989) Structure of insulin: results of joint neutron and X-ray refinement. Acta Crystallogr B 45(Pt 1):99–107

Wlodawer A, Sjolin L (1984) Application of joint neutron and x-ray refinement to the investigation of the structure of ribonuclease A at 2.0-A resolution. Basic Life Sci 27:349–364